Attention explores space periodically at the theta frequency

Mehdi Senoussi
ISAE-Supaéro, Université Fédérale de Toulouse, Toulouse, France
Present address: Department of Experimental Psychology, Ghent University, Ghent, Belgium

James C. Moreland
Department of Psychology, University of Washington, Seattle, WA, USA

Niko A. Busch
Institute of Psychology, Westfälische Wilhelms-Universität, Münster, Germany
Otto Creutzfeldt Center for Cognitive and Behavioral Neuroscience, Westfälische Wilhelms-Universität, Münster, Germany

Laura Dugué
CNRS (Integrative Neuroscience and Cognition Center, UMR 8002), Paris, France
Université Paris Descartes, Sorbonne Paris Cité, Paris, France

Voluntary attention is at the core of a wide variety of cognitive functions. Attention can be oriented to and sustained at a location or reoriented in space to allow processing at other locations—critical in an ever-changing environment. Numerous studies have investigated attentional orienting in time and space, but little is known about the spatiotemporal dynamics of attentional reorienting. Here we explicitly manipulated attentional reorienting using a cuing procedure in a two-alternative forced-choice orientation-discrimination task. We interrogated attentional distribution by flashing two probe stimuli with various delays between the precue and target stimuli. Then we used the probabilities that both probes and neither probe were correctly reported to solve a second-degree equation, which estimates the report probability at each probe location. We demonstrated that attention reorients periodically at ~4 Hz (theta) between the two stimulus locations. We further characterized the processing dynamics at each stimulus location, and demonstrated that attention samples each location periodically at ~11 Hz (alpha). Finally, simulations support our findings and show that this method is sufficiently powered, making it a valuable tool for studying the spatiotemporal dynamics of attention.

Introduction

Despite the impression that our visual perception is seamless and continuous across time, mounting evidence suggests that this is an illusion; information is sampled periodically at low frequencies (theta: 4–7 Hz; alpha: 8–12 Hz). Specifically, the alpha and theta rhythms seem to coexist in the brain and support different functions (Dugué, Beck, Marque, & VanRullen, in press; Dugué & VanRullen, 2017; Dugué, Xue, & Carrasco, 2017; VanRullen, 2016). Alpha has been related to sensory aspects of visual perception, and was first described as the natural frequency of the occipital pole (Rosanova et al., 2009). Recent studies have further proposed multiple alpha sources (i.e., occipital and parietal) serving distinct functional roles (e.g., Chaumon & Busch, 2014; Gulbinaite, van Viegen, Wieling, Cohen, & VanRullen, 2017; Sokoliuk et al., 2018). Theta appears to be related to attentional sampling (for a review, see VanRullen, 2016). Specifically, a series of recent research using exploration tasks including ones involving visual search (Dugué, Marque, & VanRullen, 2015; Dugué, McLelland, Lajous, & VanRullen, 2015; Dugué & VanRullen, 2014; Dugué, Xue, & Carrasco, 2017), priming (Huang, Chen, & Luo, 2015), exogenous (involuntary) spatial

Citation: Senoussi, M., Moreland, J. C., Busch, N. A., & Dugué, L. (2019). Attention explores space periodically at the theta frequency. *Journal of Vision*, *19*(5):22, 1–17, https://doi.org/10.1167/19.5.22.

https://doi.org/10.1167/19.5.22 Received November 27, 2018; published May 23, 2019 ISSN 1534-7362

attention (Chen, Wang, Wang, Tang, & Zhang, 2017; Landau & Fries, 2012; Landau, Schreyer, van Pelt, & Fries, 2015), endogenous (voluntary) spatial attention (Song, Meng, Chen, Zhou, & Luo, 2014), and feature-based attention (Fiebelkorn, Pinsk, & Kastner, 2018; Fiebelkorn, Saalmann, & Kastner, 2013; Helfrich et al., 2018), designed to manipulate covert attention—selective processing of information in the absence of eye movements (Carrasco, 2011, 2014)—suggests that visual information is sampled periodically at the theta frequency when attentional exploration of the visual space is required (for a review, see Dugué & VanRullen, 2017).

Recent electrophysiology in macaque monkeys and in humans using electrocorticography has shown that attention-related theta rhythm involves both sensory (V1 and V4; Kienitz et al., 2018; Spyropoulos, Bosman, & Fries, 2018) and frontal (Fiebelkorn et al., 2018; Helfrich et al., 2018) cortices. Specifically, Kienitz et al. (2018) have proposed that theta activity can emerge in sensory areas from competitive receptive-field interactions. Fiebelkorn et al. (2018) have argued instead that the theta rhythm characterizes functional interactions between the frontal eye field and the lateral intraparietal areas. Similarly, we have recently proposed that theta rhythmicity may emerge from iterative connections between sensory and attentional regions (Dugué et al., in press; Dugué & VanRullen, 2017).

Together, previous findings suggest that the periodic modulation of attentional processing in time is related to the periodic sampling of visual information in space. Attentional exploration has previously been assessed by manipulating attentional orienting and then measuring performance using a single stimulus, either at the attended location or at another, unattended location. Here we intended to clarify whether attention operates at a single location at a time, sampling sequentially across locations, or samples multiple locations simultaneously (VanRullen, 2013). To do so, we directly manipulated attentional reorienting. Reorienting is critical in a dynamic environment that changes rapidly at short timescales, along with observers' goals and priorities. Characterizing the dynamics of attention's ability to shift and enhance vision across multiple points of interest is crucial for understanding the limits and capacity of the visual system. Importantly, there is no reason to assume that endogenous orienting (i.e., voluntary engagement of attention on a given spatial location) behaves equally to endogenous reorienting (i.e., first necessitating disengagement of the attention focus from one location to shift and reengage onto another location; Posner, 1988).

Recently, Dugué, Roberts, and Carrasco (2016) used transcranial magnetic stimulation (TMS) to directly assess the interplay between temporal periodicity and sequential spatial exploration. They investigated the dynamics of endogenous (voluntary) spatial attention. Using a cuing procedure, they explicitly manipulated attentional orienting—attending to one location within a trial—and reorienting—shifting attention from one stimulus location to another, previously unattended location (Corbetta, Patel, & Shulman, 2008; Dugué, Merriam, Heeger, & Carrasco, 2017). By applying TMS at various delays over the occipital pole (V1/V2), they demonstrated that performance in a two-alternative forced-choice (2-AFC) orientation-discrimination task was modulated by occipital TMS periodically at the theta frequency (~5 Hz) only when attention had to be reallocated from a distractor to a target location. However, due to practical considerations tied to the use of TMS, the frequency resolution was not optimal for allowing precise characterization of the peak frequency of attentional reorienting (eight stimulation delays on a 400-ms window).

Here we investigated the spatial and temporal dynamics of attentional sampling by explicitly manipulating attentional reorienting. In a psychophysical task, we probed the state of attentional allocation during the course of the trial with high temporal resolution. Two probes were flashed at various delays after the offset of two grating patches. Participants performed a 2-AFC orientation-discrimination task on one of the two grating patches, with voluntary attentional orienting and reorienting manipulated using a central cue. Assessing performance on the probes, we used a probability-estimation method that consisted of solving a second-degree equation using the probabilities that both probes and neither probe were correctly reported to estimate the amount of attention allocated to the different stimulus locations over time. Critically, by manipulating the probe configuration we were able to analyze both attentional reorienting between stimulus locations and information sampling at each location independently. This approach—first introduced by Dubois, Hamker, and VanRullen (2009) and then successfully applied to investigate the spatiotemporal deployment of attention during visual search (Dugué, McLelland et al., 2015; Dugué, Xue, & Carrasco, 2017)—allowed us to demonstrate that attentional distribution was periodically modulated over time at the theta frequency (~4 Hz) only when attention had to be reoriented. Through our explicit manipulation of the reorienting of endogenous attention and use of a fine-tuned psychophysical and analytical approach, these results suggest that the periodicity in task performance was due to the sequential reorienting of attention from one stimulus location to another, and not the independent sampling of either location. Importantly, our method allowed us to also show that each stimulus location was processed periodically at the alpha frequency (~11 Hz), suggesting a functional dissociation between the alpha and theta rhythms.

Methods

Observers

Thirteen human observers (nine women, four men; age [$M \pm SD$] = 20.9 ± 0.8 years; range: 20–22) were recruited for this experiment—prior studies using the same analysis approach have had a similar number of participants (Dugué, McLelland et al., 2015; Dugué, Xue, & Carrasco, 2017). The decision to stop recruiting new observers was not based on preliminary analyses of the data. We selected a study design in which each participant undertook a large number of trials (1,872 trials total). Due to technical issues during data recording, two observers were excluded from the analysis. All observers had normal or corrected-to-normal vision. They provided written informed consent and received monetary compensation for their participation. All procedures were approved by the CERES (Conseil d'Évaluation Éthique pour les Recherches En Santé) ethics committee of Paris Descartes University. All research was performed in accordance with the relevant guidelines and regulations from the committee.

Apparatus

Observers sat in a dark room, 57.5 cm from a calibrated and linearized CRT monitor (refresh rate: 85 Hz; resolution: 1,280 × 1,024 pixels). A chin rest was used to stabilize head position and distance from the screen. Visual stimuli were generated and presented using MATLAB (MathWorks, Natick, MA) and the MGL toolbox (http://gru.stanford.edu/doku.php/mgl/overview).

Procedure

Data collection took place across five sessions conducted on five consecutive days. Note that the collected data sets are available through an Open Science Framework repository (https://osf.io/2d9sc/?view_only=6ef3f85d9f944d27b23fc7af5a26f087). MATLAB code to replicate the experiment, analyses, and figures are provided through GitHub (https://github.com/mehdisenoussi/PECAR). The first session was used to familiarize observers with the experimental protocol. In the four remaining 1-hr sessions, observers performed the main task.

Observers performed a 2-AFC orientation-discrimination task as depicted in Figure 1A. They were instructed to fixate on a white cross at the center of the screen. Eye position was monitored using an infrared video-camera system (EyeLink 1000, SR Research, Ottawa, Canada) to ensure that all observers maintained fixation throughout each trial (critical when studying covert attention). Stimulus presentation was contingent upon fixation. Any trials in which observers broke fixation (defined as an eye movement ≥1.5° from the center of the fixation cross, or as blinking; $M \pm SD$ = 15% ± 8%) were canceled and then repeated at the end of each experimental block. Note that eye movements ≤1.5° from the center of the fixation cross (i.e., microsaccades) were not detected online. However, a post hoc analysis showed that these were inconsequential ($M \pm SD$ = 0.05 ± 0.01 microsaccade per trial when considering the period between the offset of the grating stimuli and the onset of the probes; see later).

A central endogenous precue presented for 50 ms instructed observers to deploy their covert attention toward the left or right bottom quadrant. The precue was followed by a 350-ms interstimulus interval—sufficient time to deploy voluntary attention (Busse, Katzner, & Treue, 2008; Carrasco, 2011; Cheal & Lyon, 1991; Dugué, Merriam, et al., 2017; Liu, Stevens, & Carrasco, 2007; Müller & Rabbitt, 1989; Nakayama & Mackeben, 1989; Pestilli, Ling, & Carrasco, 2009). Two stimuli were then presented for 60 ms: sinusoidal gratings windowed by a raised cosine (15% contrast, 3 c/°, at 4° eccentricity, on a gray background). They were tilted randomly clockwise or counterclockwise relative to the vertical. The tilt angle was chosen for each individual via a staircase procedure performed during the first session using a neutral precue (two precues: one pointing to the right and the other one to the left quadrant, half the size of the single precue) to achieve ~75% accuracy (average [$M \pm SD$] tilt angle = 7.02° ± 4.02°) independently for all observers. The target grating—that is, the stimulus for which observers had to report the orientation—was indicated by a central response cue pointing toward either the left or the right bottom quadrant. Two gratings were always presented, one for each quadrant (in each quadrant the location was randomly selected from one of five possible locations, as depicted in Figure 1B). A trial was valid when the quadrant in which the target grating appeared matched the precued quadrant (75% of the trials). A trial was invalid when the target appeared at the uncued quadrant (25% of the trials), requiring reorienting attention endogenously to the opposite quadrant. For each participant there were a total of 1,404 valid and 468 invalid trials. Note that for all analyses we used all available trials. However, to ensure that any observable difference between the valid and invalid trials is not due to the different number of trials, we also performed the main analysis (Figure 2, left column) by subsampling for each participant the number of valid trials to match it with the number of invalid trials—that is, for the valid-trial condition only,

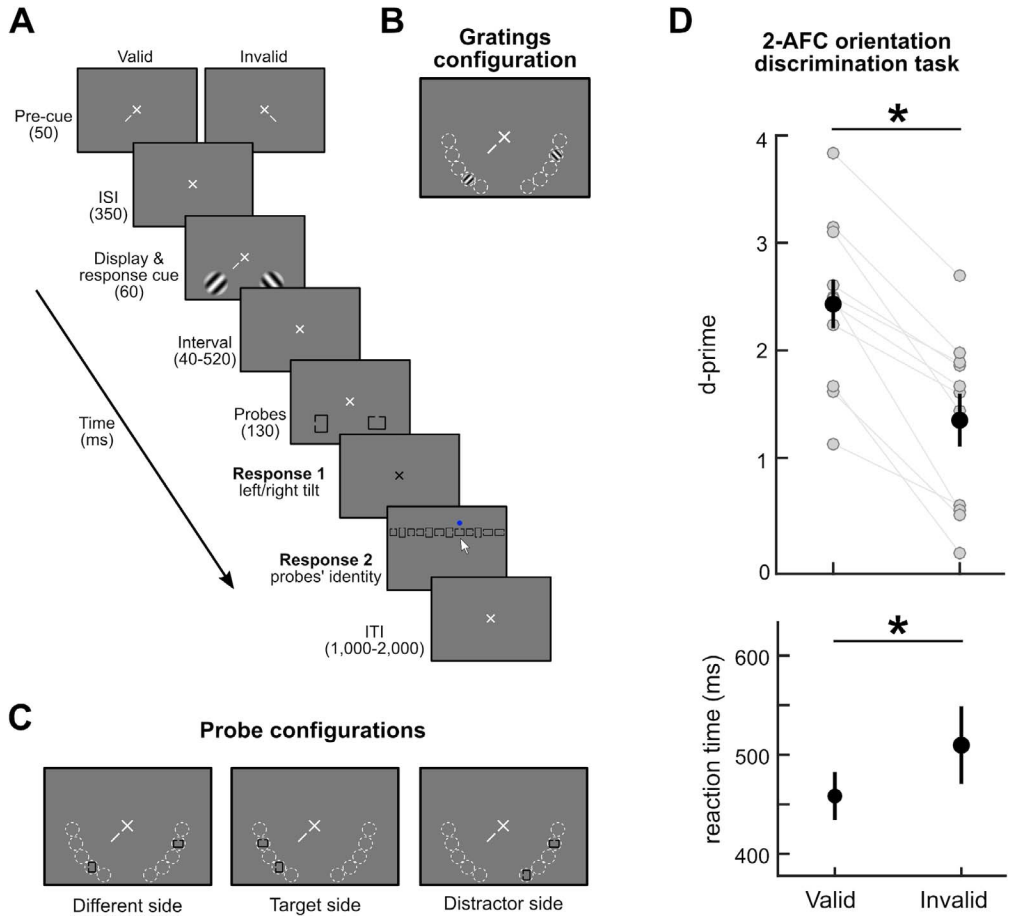

Figure 1. Experimental protocol. (A) Trial sequence: Each trial consists of precuing, a two-alternative forced-choice orientation-discrimination task, and a probe-identification task. (B) In each quadrant, the grating appeared in one of five possible positions represented by the dashed white circles (the circles are for illustration purposes only and were not present in the actual experiment). (C) The probes appeared in one of three possible configurations: one probe in each quadrant or both probes on the same side as either the target or the distractor grating. (D) Performance in the two-alternative forced-choice orientation-discrimination task. Top panel: d' as a function of validity condition (valid or invalid). Each gray dot represents an individual observer. Black dots represent the average across observers. Error bars reflect ± 1 standard error of the mean. Values of d' are significantly higher in the valid than the invalid condition, $t(10) = 7.57$, $p < 0.0001$, Cohen's $d = 1.368$. Bottom panel: Median reaction time across observers. Error bars reflect ± 1 standard error of the mean. Reaction times are significantly faster in the valid than the invalid condition, $t(10) = -2.54$, $p = 0.031$, Cohen's $d = 0.479$. Results confirm that attention was successfully manipulated, with no speed/accuracy trade-off.

we reran the analysis on 468 randomly selected valid trials (1,000 iterations)—and found similar results.

Two Landolt Cs—squares or rectangles with an aperture on one of the sides (12 possible probes: four squares, four horizontal rectangles, and four vertical rectangles)—were presented for 130 ms after one of 13 possible delays after the onset of the orientation-discrimination display (interstimulus interval: 40–520 ms, in 40-ms increments; 144 trials per delay). Upon offset of the probes, the fixation cross turned black to indicate the beginning of the response window during which observers had to report the tilt orientation of the target (clockwise or counterclockwise to vertical). Auditory positive (high tone) or negative (low tone) feedback was provided to the observers. We calculated d' to measure accuracy as our main dependent variable. To rule out any speed/accuracy trade-offs, we also report median reaction time from the onset of the response window as a secondary dependent variable. The fixation cross disappeared after the observers responded, and a horizontally aligned array of the 12 possible probes appeared. The order of the probes' identity in the array was randomized between trials. Observers used the computer mouse to report probe identity by clicking on each of the two probes they perceived (see Figure 1A). When observers clicked on a given probe in the array, a blue dot appeared for 500 ms above the probe to indicate that it was selected. It was possible for the two probes to be identical (observers were aware of this possibility), in which case observers had to click twice on the same probe. There was no feedback for performance on the probe task, in

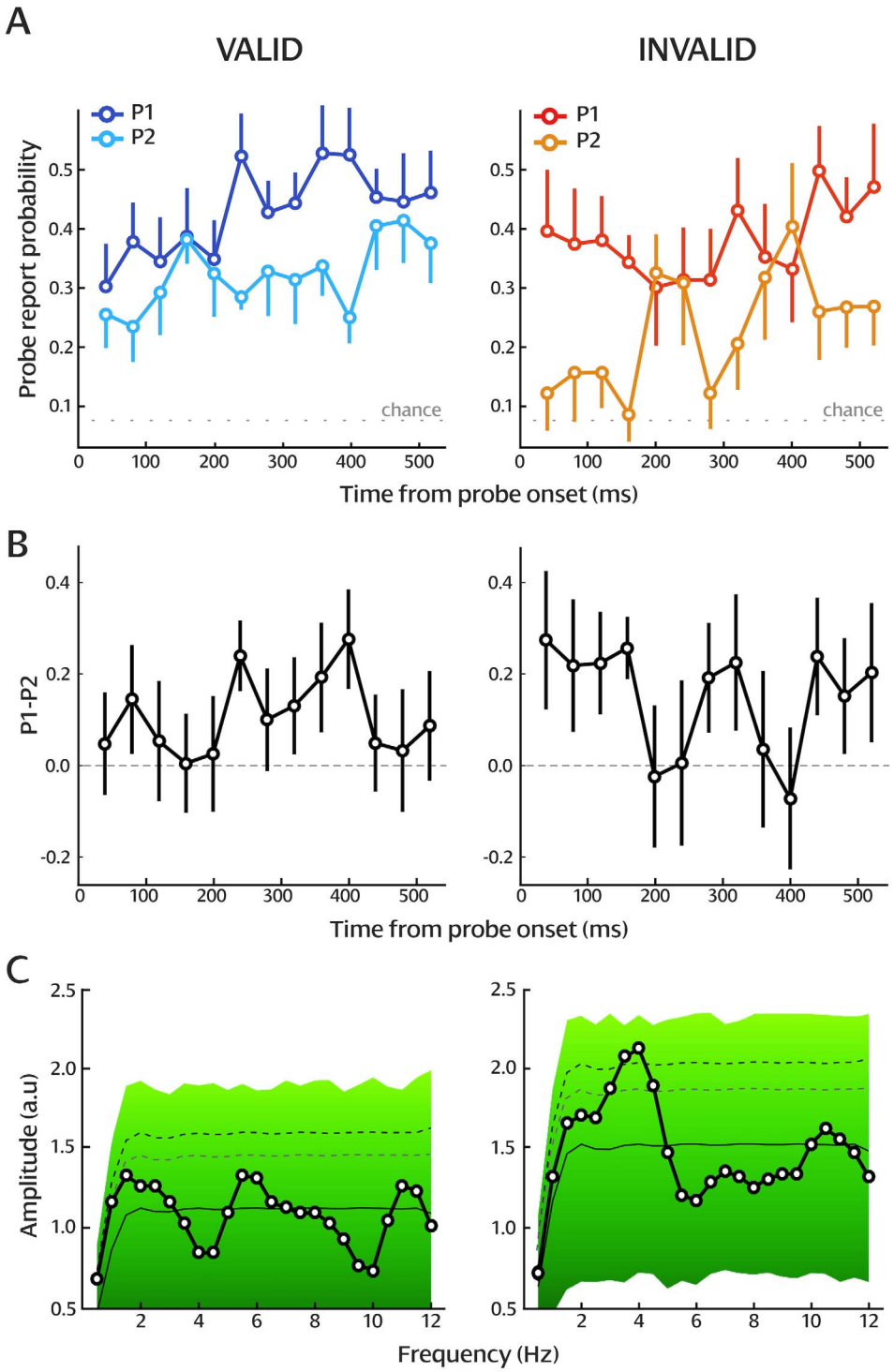

Figure 2. Dynamics of attentional orienting and reorienting. (A) P_1 and P_2 by delays for the valid (left column) and invalid (right column) conditions (probability estimation from the probe task). The dotted line represents the probability of correctly reporting the probe by chance (0.083). Error bars reflect ± 1 standard error of the mean. Only one half of the error bars are shown, to reduce visual clutter. (B) Difference between P_1 and P_2. The dashed line represents zero difference. Error bars reflect ± 1 standard error of the mean. (C) Amplitude spectrum of the difference between P_1 and P_2 and results of the 100,000-surrogate analysis for the valid and invalid conditions. In each graph, the solid line represents the average of the surrogate analysis. The black-to-green background represents the distribution of surrogate values—that is, the level of significance of each frequency component. The gray dashed line represents $p < 0.05$. The black dashed line represents $p < 0.05$ after Bonferroni correction.

order to ensure that observers prioritized the first task. For each trial, we recorded whether the observer reported neither, one, or both probes correctly.

There were three probe-location conditions: the two probes were presented in opposite quadrants (randomly located in one of the five possible locations within the quadrant; Figure 1C, left panel) or both in the same quadrant as either the target (Figure 1C, middle panel) or the distractor (opposite side; Figure 1C, right panel). The analysis performed on trials in which one probe was presented in each quadrant assayed attentional reorienting, whereas the analysis performed on the other two conditions concerned information sampling at each location. All analyses were performed on trials in which observers correctly responded in the 2-AFC task (grating orientation), to ensure that they followed the primary task's instructions and that attention was successfully deployed to the target location. Crucially, the Landolt Cs were used to probe the state of attentional distribution (see Probability estimates). Specifically, this manipulation allows interrogation of the spatial location of the attention focus at various delays over the course of the trial. Note that our approach allowed us to determine whether both probes received the same amount of attention or one received more than the other one on average across all trials. We remain agnostic of the exact location of the attentional focus on a trial-by-trial basis.

Probability estimates

We aimed to investigate the spatiotemporal behavior of attention during a task in which we explicitly manipulated the orienting and reorienting of endogenous attention. Specifically, performance to identify the two probes presented at different locations shortly after the gratings informs us on how attention was differentially distributed in the visual field. In other words, we asked whether attention is sampling both probe locations equally at each time point or whether the distribution of attentional resources between probe locations is modulated over time, suggesting that attention alternates between probe locations in time.

To examine this question, we used the method previously introduced by Dubois et al. (2009) and then successfully applied in visual search tasks by Dugué and colleagues (Dugué, McLelland et al., 2015; Dugué, Xue, & Carrasco, 2017) to characterize attentional deployment. This probability-estimation method allows extraction of an estimate of attentional distribution when the location of attention is unknown. Note that in our experiment we have two types of probe configurations: Both probes were presented either in the same quadrant or in opposite quadrants. Our paradigm allows access to the relative attentional distribution between quadrants over time (cued vs. uncued quadrant) but not within a quadrant (five possible stimulus positions). We thus used a probability-estimation method able to estimate attentional distribution for all probe configurations.

The probabilities of attending to each of the probed locations called P_1 (probability of reporting the probe at the most attended location) and P_2 (probability of reporting the probe at the least attended location), were determined using the probabilities of reporting both probes correctly—P(both)—and neither probe correctly—P(none).

The probability of getting both probes correct is

$$P(\text{both}) = P_1 \times P_2 \rightarrow P_1 = \frac{P(\text{both})}{P_2}. \quad (1)$$

Note that the relation of independence between the probes is ensured by the task allowing them to be identical (i.e., the choice of the second probe does not depend on the choice of the first one).
The probability of getting neither correct is

$$\begin{aligned} P(\text{none}) &= (1 - P_1)(1 - P_2) \rightarrow P(\text{none}) \\ &= 1 - P_1 - P_2 + P_1 \times P_2. \quad (2) \end{aligned}$$

Substituting Equation 1 into Equation 2 yields

$$P(\text{none}) = 1 - \frac{P(\text{both})}{P_2} - P_2 + \frac{P(\text{both})}{P_2} \times P_2. \quad (3)$$

Moving all to one side of the equation gives

$$\begin{aligned} 0 = 1 - P(\text{none}) - \frac{P(\text{both})}{P_2} - P_2 \\ + \frac{P_2 \times P(\text{both})}{P_2}. \quad (4) \end{aligned}$$

Multiplying all by $-P_2$ yields

$$\begin{aligned} 0 = -P_2 + P(\text{none}) \times P_2 + P(\text{both}) + {P_2}^2 \\ - \frac{{P_2}^2 \times P(\text{both})}{P_2}. \quad (5) \end{aligned}$$

And rearranging finally gives

$$\begin{aligned} 0 = {P_2}^2 - P_2 + P(\text{none}) \times P_2 - \frac{{P_2}^2 \times P(\text{both})}{P_2} \\ + P(\text{both}) \quad (6) \end{aligned}$$

$$\begin{aligned} 0 = {P_2}^2 - P_2 \times (1 - P(\text{none}) + P(\text{both})) \\ + P(\text{both}) \quad (7) \end{aligned}$$

$$0 = {P_2}^2 - P_2 \times \Sigma + \Pi, \quad (8)$$

with $\Pi = P(\text{both})$ and $\Sigma = 1 - P(\text{none}) + P(\text{both})$.

Equation 8 is now quadratic and can be solved using the quadratic formula for P_2. Because P_1 and P_2 are

symmetric in these equations, the two solutions of Equation 8 are P_1 and P_2.

Calculating the discriminant Δ as follows will allow us to solve Equation 8:

$$\Delta = \Sigma^2 - 4 \times \Pi. \quad (9)$$

The solutions of Equation 8 are then

$$P_1 = \frac{\Sigma + \ \text{sign}(\Delta) \times \ \sqrt{|\Delta|}}{2}$$

$$P_2 = \frac{\Sigma - \text{sign}(\Delta) \times \ \sqrt{|\Delta|}}{2}.$$

Note that due to noise in responses and performance, and a relatively low number of trials per condition, negative values of Δ were sometimes obtained, which can produce nonreal solutions. To address this problem, we followed the same approach as Dugué and colleagues (Dugué, McLelland et al., 2015; Dugué, Xue et al., 2017) and used $|\Delta|$ and sign(Δ), thus allowing P_1 and P_2 values to be negative.

Evaluating the mathematical approach to calculate attentional distribution

For comparison purposes with the results of the previous studies, we present the results as a function of P_1 and P_2 using the absolute value and the sign of the discriminant (see previous section). As developed in the previous studies, this is a more conservative solution than assigning a zero value to Δ or taking its absolute, which would artificially increase differences between P_1 and P_2. This approach also has the advantage of giving a straightforward, intuitive interpretation—that is, if P_1 equals P_2, then both probe locations received the same amount of attention; however, if P_1 is greater than P_2, then one location received more attention than the other one.

To further test our probability estimates, we also performed the analysis of the discriminant. As shown later, the discriminant is the square of the difference between P_1 and P_2 in the case where coefficient $a = 1$, and is an unbiased estimate.

Beginning with the quadratic formula,

$$(P_1, P_2) = \frac{\Sigma \pm \sqrt{\Delta}}{2},$$

we can subtract the negative solution from the positive to describe $P_1 - P_2$:

$$P_1 - P_2 = \frac{\Sigma + \sqrt{\Delta}}{2} - \frac{\Sigma - \sqrt{\Delta}}{2},$$

which reduces to

$$P_1 - P_2 = \frac{2 \times \sqrt{\Delta}}{2}$$

$$(P_1 - P_2)^2 = \Delta.$$

This means that the discriminant as it was used in the analyses of the previous studies is equal to $(P_1 - P_2)^2$ before the absolute value was taken. If there is no difference between the probability of reporting either probe, then $P_1 - P_2 = 0$, and so will the discriminant: $(P_1 - P_2)^2 = 0$. If performance on one probe depends on the other, and correctly reporting one makes reporting the other correctly less likely, then the discriminant will scale (nonlinearly) with the size of this difference.

Spectral analysis

To analyze the temporal dynamics of attentional distribution in valid and invalid conditions, we computed a fast Fourier transform (FFT—we decomposed the behavioral data from the time domain into frequency components to estimate an amplitude spectrum, i.e., the amount of each frequency present in the original data; e.g., Chota et al., 2018; Dugué, McLelland et al., 2015; Dugué et al., 2016; Dugué, Xue, & Carrasco, 2017; Fiebelkorn et al., 2013; Ho, Leung, Burr, Alais, & Morrone, 2017; Landau & Fries, 2012; Song et al., 2014; Zhang, Morrone, & Alais, 2019), for each observer, on the difference between P_1 and P_2, and then averaged the resulting amplitude spectra across observers. Note that here we did not analyze the absolute values of P_1 and P_2. Instead, we were interested in the difference between P_1 and P_2, which represents the relative distribution of attention across the two probes regardless of their actual location—that is, a difference of zero indicates that both probe locations received the same amount of attentional resources (uniform attentional distribution), while a positive difference indicates that one probe location received more resources than the other (nonuniform attentional distribution).

The data of each observer were average-padded to increase the frequency resolution—that is, values corresponding to the average of the difference between P_1 and P_2 across delays were added on either side of the empirical data points. Specifically, the 13 time points, spanning 480 ms, were padded to get a 2,000-ms segment, thus adding 18 data points before the first data point and 19 after the last one. Note that we also performed the analysis on nonpadded data and obtained similar results.

To calculate statistical significance of each frequency component, we used permutation tests (100,000 surrogates of the index for each participant), under the null

hypothesis of a random temporal structure of the difference between P_1 and P_2. We shuffled the delays, padded the data as just described, and computed the FFT over each surrogate. The amplitudes of the surrogate FFT results were then sorted in ascending order. We used a statistical threshold at $p < 0.05$, corrected for multiple comparisons (six frequency components corresponding to the true frequency resolution of the difference between P_1 and P_2) using Bonferroni correction (833rd highest value; in other words, $p < 0.00833$).

Finally, in addition to the probability-estimation method that we used to investigate the temporal dynamics of attentional distribution within and between quadrants, we analyzed the temporal dynamics of probe-report accuracy for trials in which one probe appeared in each quadrant (Figure 2C, left panel). For these trials, we computed the FFT for each observer on the difference between probe-report accuracy in the attended quadrant (indicated by the precue) and in the unattended quadrant, and then averaged the resulting amplitude spectra across observers. We again padded to the average, and significance was calculated by shuffling the probe-report accuracy difference across delays.

Results

Grating task

We first evaluated the performance in the 2-AFC orientation-discrimination task (Figure 1D) in order to ensure that observers correctly performed the task and that attention was successfully manipulated. We computed d' for reporting the tilt orientation of the target grating in the valid and invalid conditions and observed significantly higher sensitivities for the valid than the invalid condition (two-tailed, paired-sample t test), $t(10) = 7.57$, $p < 10^{-4}$, 95% confidence interval (CI) [0.76, 1.4], Cohen's $d = 1.368$. There was also a significant difference in median reaction time between the valid and invalid conditions: Observers responded faster in the valid condition, $t(10) = -2.54$, $p = 0.031$, 95% CI [−0.10, −0.006], Cohen's $d = 0.479$. Both variables reflected an attentional facilitation in the 2-AFC orientation-discrimination task, demonstrating that attention was successfully manipulated, with no speed/accuracy trade-offs.

Probe task

We measured performance in reporting both probes—P(both)—and neither of the probes—P(none)—correctly. To investigate the dynamics of attentional reorienting, we used P(both) and P(none) to estimate probe-report probabilities for the condition in which the probes were presented in opposite quadrants (see Methods). We observed that P_1 and P_2 were marginally significantly different in the valid condition (two-way repeated-measures analysis of variance), $F(1, 10) = 4.405$, $p = 0.062$, $\eta^2 = 0.30$ (Figure 2A, left panel). This difference was significant in the invalid condition, $F(1, 10) = 22.976$, $p = 0.0007$, $\eta^2 = 0.69$ (Figure 2A, right panel). Both were well above chance (chance in probe-report probability = 0.083). We argue that attention in the probe task was nonuniformly distributed across the two stimulus locations.

To assess the temporal dynamics of attentional distribution, we calculated the difference between P_1 and P_2 (Figure 2B) separately for valid and invalid trials. We then performed an FFT on the difference for each observer and analyzed the resulting averaged amplitude spectra (Figure 2C; see Methods). In the valid condition there was no significant peak frequency. In the invalid condition there were significant peaks at 3.5 and 4 Hz ($p < 0.05$, Bonferroni corrected), suggesting that the difference between P_1 and P_2 for each observer was modulated periodically at the theta frequency.

To further validate our results, we compared the valid and invalid conditions (Figure 3A) for the difference between P_1 and P_2 and replicated it on the discriminant (see Methods). For the difference, the amplitude of the 4-Hz component for each observer was significantly higher in the invalid than the valid condition (one-tailed, paired-sample t test), $t(10) = 3.86$, $p = 0.001$, 95% CI [0.5296, 1.977], Cohen's $d = 1.647$, consistent with the results of Figure 2C. For the discriminant, the amplitude of the 4-Hz component was also significantly higher for the invalid than the valid condition (Figure 3B; one-tailed, paired-sample t test), $t(10) = 3.36$, $p = 0.004$, 95% CI [0.2691, 1.3298], Cohen's $d = 1.383$, confirming the validity of our method.

To assess the temporal dynamics of attentional distribution, we estimated probe-report probability at the most (P_1) and least (P_2) attended location using the analysis approach described under Methods, which is agnostic to the actual probe location. However, because of our cuing manipulation, we know which probe is presented in the attended quadrant (i.e., quadrant indicated by the precue) and which one is presented in the unattended quadrant. To confirm the results from the previous analysis, we thus performed the same spectral decomposition directly on the difference in probe-report accuracy between the attended and unattended quadrants, taking again only trials in which the probes appeared in opposite quadrants (Figure 4; see Methods). In the valid

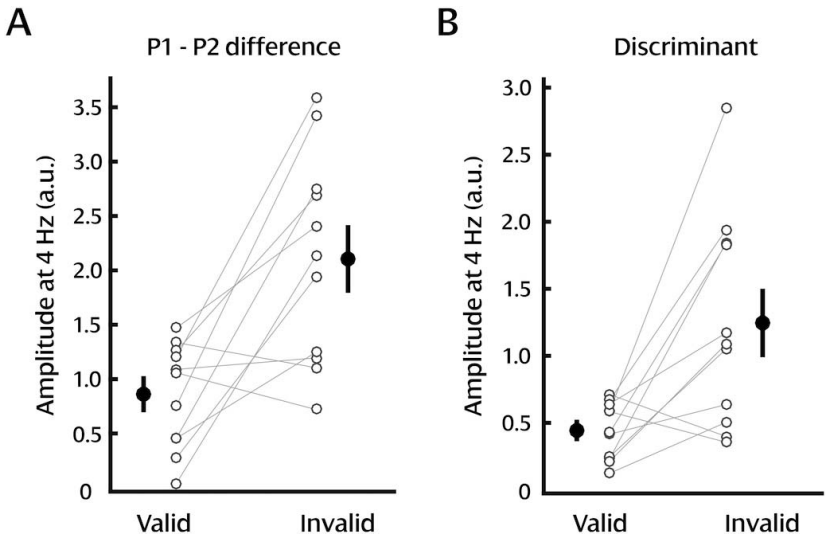

Figure 3. Analysis comparison. A fast Fourier transform was performed for each observer separately for both (A) the difference between P_1 and P_2 and (B) the discriminant, for the valid and invalid conditions. Empty black circles represent the amplitude of the 4-Hz component for individual observers. Black filled circles represent the average across observers. Error bars reflect ± 1 standard error of the mean. The difference between valid and invalid conditions was significant for both the difference between P_1 and P_2, $t(10) = 3.86$, $p = 0.001$, Cohen's $d = 1.647$, and the discriminant, $t(10) = 3.36$, $p = 0.004$, Cohen's $d = 1.383$.

condition, there was no significant peak in frequency (Figure 4A). In the invalid condition, there was a significant peak at 3 Hz (Figure 4B; $p = 0.022$, although it does not withstand Bonferroni correction), in line with the periodic modulation previously observed in the difference between P_1 and P_2 (3.5–4 Hz; Figure 2C).

Note that this effect is not as strong as the one obtained using the probability-estimation method. As described in Figure 1C left panel, the probe could appear at five possible positions in the attended or unattended quadrant, and potentially at a different location from the grating in the quadrant. For both analyses, we combined all trials together, regardless of the actual location of the probe within each quadrant. The probability-estimation method is insensitive to specific probe location—that is, it estimates the relative attentional distribution across spatial locations. However, when examining probe-report accuracies, we estimated the absolute probability of reporting a single probe, which is arguably influenced by the specific stimulus configuration.

Critically, to investigate attentional distribution within each quadrant we analyzed trials in which both probes were presented in the same quadrant as the target or the distractor (Figure 1C, middle and right panels). In this case, analyzing probe-report accuracies cannot inform the attentional distribution within the quadrant since we do not know where attention is allocated within the quadrant—an entire quadrant was precued on each trial. Thus, we need to use the probability-estimation method. Specifically, we performed the same analysis as in Figure 2C for trials in which both probes were presented in the same quadrant—that is, same side as the target or the distractor. Note that here we used the probability-estimation method to evaluate, in each quadrant, whether one probe was processed more efficiently than the other one, independently of our manipulation of attentional distribution. The results show a significant effect in the valid-trial condition at low frequencies ($<$1.5 Hz; $p < 0.0234$, although it does not withstand the Bonferroni correction; Figure 5A). This effect presumably corresponds to a slow trend in the difference between P_1 and P_2 over the course of the trial, and not a true periodic modulation. In the invalid-trial condition, we observe a significant periodic modulation of the difference between P_1 and P_2 at the alpha frequency (10–11 Hz; $p = 0.03$, although it does not withstand the Bonferroni correction; Figure 5B). We finally show that this periodic modulation at the alpha frequency is present for both trials in which the probe appears in the same quadrant as the target (10 Hz; $p = 0.0110$, although it does not withstand the Bonferroni correction; Figure 5C, top panel) and trials in which the probe appears in the same quadrant as the distractor (11 Hz; $p = 0.0074$; Figure 5C, bottom panel).

Power analysis

The sequential-attentional-reorienting interpretation of the results suggests that within a trial, the probability of detecting the probe's identity is dependent across locations—that is, if the observers correctly identify a

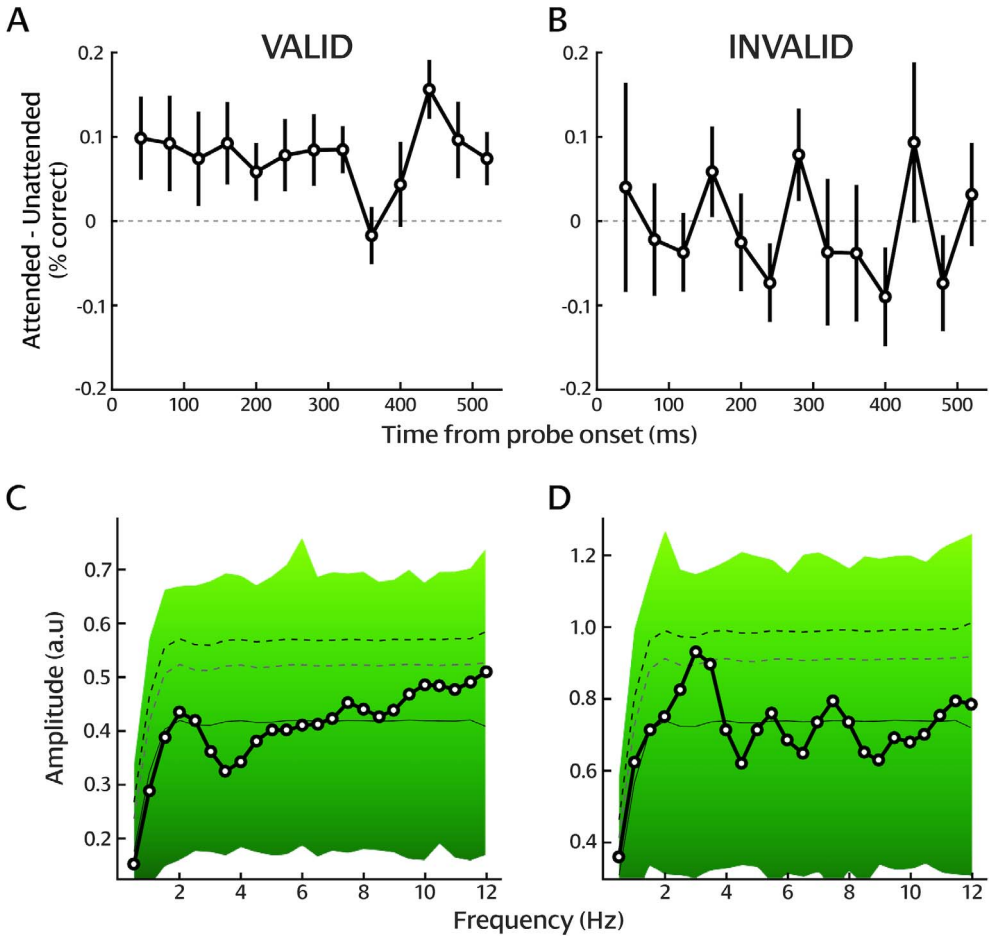

Figure 4. Dynamics of attentional distribution measured using probe-report accuracies. (A–B) Difference between attended (indicated by the precue) and unattended probe-report accuracies for (A) valid and (B) invalid trials. The dashed line represents a zero difference. Error bars reflect ±1 standard error of the mean. (C–D) Amplitude spectra of the difference in probe-report accuracy between trials in which the probes appeared in the attended and unattended quadrant, for (C) valid and (D) invalid trials, and results of the 100,000-surrogate analysis. The solid line represents the average of the surrogate analysis. The black-to-green background represents the distribution of surrogate values—that is, the level of significance of each frequency component. The gray dashed line represents $p < 0.05$. The black dashed line represents $p < 0.05$ after Bonferroni correction.

probe at one location, they are less likely to identify the probe at another. This dependency is lost if the probe responses to one location are randomly permuted. The result is the same overall percent correct for each probe, but probe responses within each trial are independent.

To evaluate the statistical power of the probability-estimation method, we tested the null hypothesis of no dependency between the two probe responses within a trial. We generated a surrogate distribution under this null hypothesis by repeatedly (10,000 repetitions) permuting the probe responses at one location and performing the quadratic analysis on the resulting pairs of probe responses. This null distribution was then compared to a distribution generated by resampling trial responses with replacement while preserving any existing dependency within a trial (Figure 6). The achieved power is the proportion of sampling repetitions from the distributions of resampling difference between P_1 and P_2 (Figure 6A and 6B) and discriminant (Figure 6C and 6D) that are greater than the 95th percentile of the permuted distributions. For the difference between P_1 and P_2, the achieved power was 99.4% in the valid condition and 10.5% in the invalid condition. For the discriminant, the achieved power was 100% in the valid condition and 34.4% in the invalid condition. Interestingly, the permuted data do not have a discriminant distribution centered on zero, as would be expected if there were no relation between the two probe responses. A possible explanation is that observers had a bias in performance for the first or second probe response, which is a relation preserved in the permutation method.

In conclusion, using this power analysis we addressed the question whether the quadratic analysis approach is sufficiently powered to detect a difference between the probabilities of correctly reporting probe

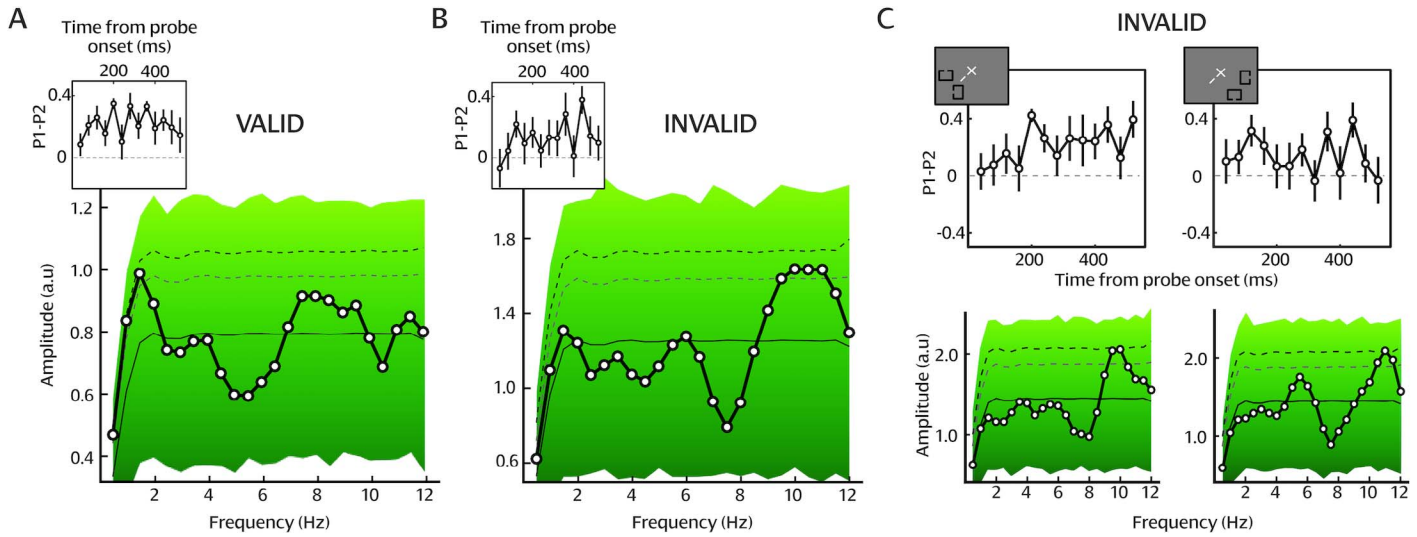

Figure 5. Dynamics of information processing in each visual quadrant. (A–B) Difference between P_1 and P_2, corresponding amplitude spectra, and results of the 100,000-surrogate analysis for (A) valid- and (B) invalid-trial conditions. (C) The same analysis presented for the invalid-trial condition separately for trials in which both probes are presented on the target side (left panel) and trials in which both probes are presented on the distractor side (right panel). In each graph of the difference between P_1 and P_2, the dashed line represents zero difference and error bars reflect ± 1 standard error of the mean. In each of the graphs of the amplitude spectra, the solid line represents the average of the surrogate analysis. The black-to-green background represents the distribution of surrogate values—that is, the level of significance of each frequency component. The gray dashed line represents $p < 0.05$. The black dashed line represents $p < 0.05$ after Bonferroni correction.

one and probe two. Based on the permutation tests (Figure 6), we were able to conclude that this method is appropriate and sufficiently powered to detect such a difference. This assessment adds support to the literature already published (Dubois et al., 2009; Dugué, McLelland et al., 2015; Dugué et al., 2016).

Discussion

We investigated the spatiotemporal dynamics of attentional orienting and reorienting using a psychophysical approach with high temporal resolution. By explicitly manipulating covert spatial, endogenous attention, we demonstrated that performance in the invalid condition, when attention needed to be reoriented from the distractor to the target location, was periodically modulated at the theta frequency (~4 Hz; Figures 2 and 4). Additionally, we found that stimuli presented in the same quadrant were sampled periodically at the alpha frequency (~11 Hz; Figure 5; see also Figure 7). Finally, we performed our analysis on another index of attentional distribution—the discriminant (Figure 3)—and replicated the effect.

Interestingly, our probability-estimation approach allowed us to investigate not only the rhythm of attentional reorienting but also the rhythm of information sampling at each location. We found a functional dissociation between the theta rhythm, observed in analyzing trials in which the probes were presented in opposite quadrants, and the alpha rhythm, observed in analyzing trials in which both probes were presented in the same quadrant. Specifically, our results suggest that the alpha and theta rhythms jointly allow periodic sampling of the visual environment. The ongoing alpha rhythm—that is, sensory rhythm (~11 Hz; whose phase may not be reset by stimulus onset, or only partially)—would coexist with the theta attentional rhythm (~4 Hz) and either be recordable concurrently or be masked depending on task relevance. This is consistent with recent literature reviews suggesting that theta corresponds to the rhythm of attentional exploration while alpha reflects an ongoing, sensory sampling rhythm (Davidson, Alais, van Boxtel, & Tsuchiya, 2018; Dugué & VanRullen, 2017; VanRullen, 2016).

Recent studies have shown that interactions between frequency bands are critical for the brain to orchestrate different aspects of visual and attentional processing (Helfrich, Huang, Wilson, & Knight, 2017; Klimesch, 2018). Specifically, Helfrich et al. (2017) observed that phase-amplitude cross-frequency coupling between oscillations at 2–4 Hz and at 8–12 Hz—that is, the phase of the oscillations at 2–4 Hz modulates the amplitude of those at 8–12 Hz—alters behavioral performance in a visual-detection task. Here, because theta and alpha behavioral rhythms were revealed in different conditions, we were not able to test for a

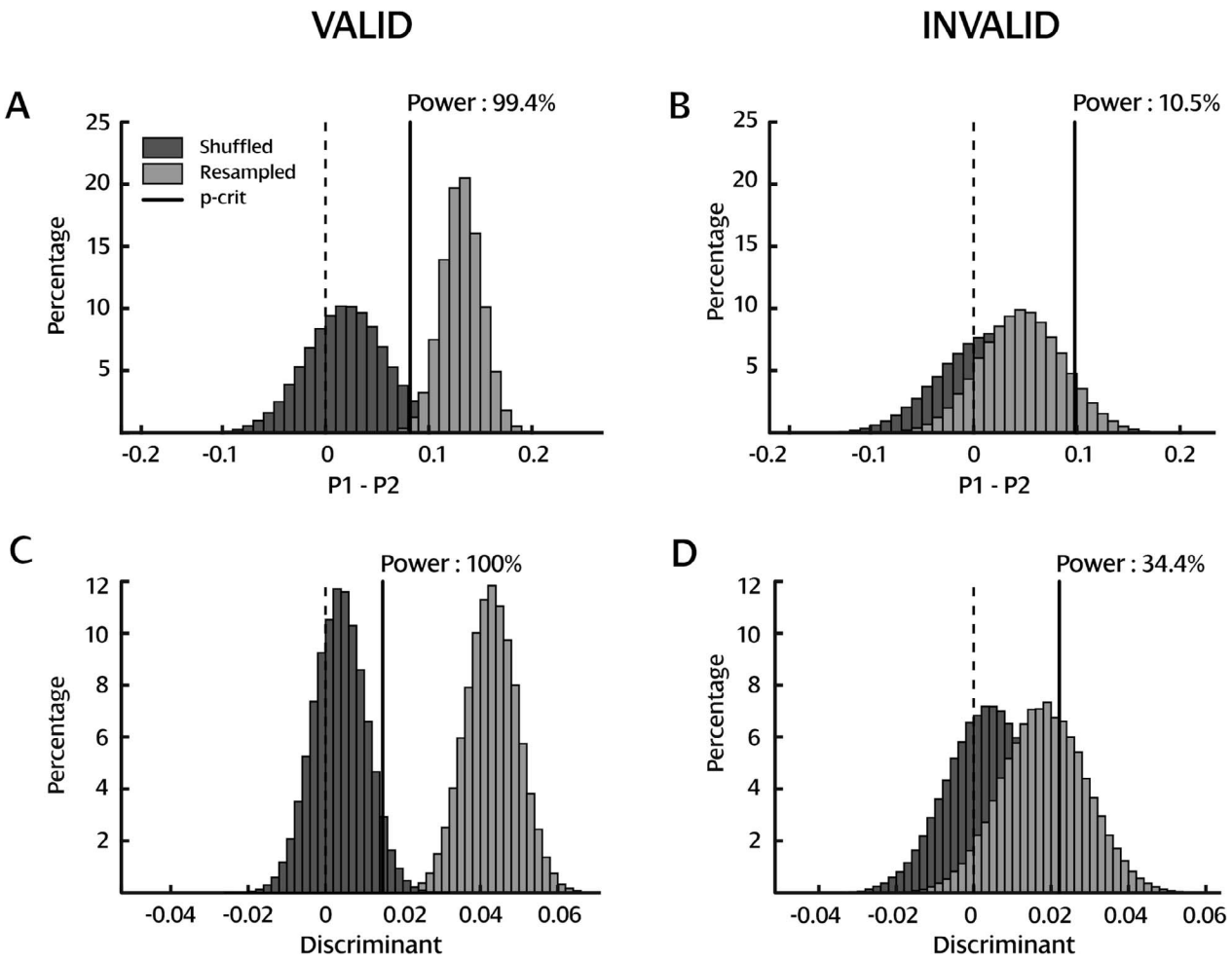

Figure 6. Power analysis. Distributions of the difference between P_1 and P_2 and discriminant for resampled and permuted trials, for the valid (left panels) and invalid (right panels) conditions. Solid vertical lines in each panel indicate the 95th percentile of the permuted distribution. The proportion of resampled repetitions to the right of the solid line indicates the power achieved.

potential interaction, and further research will be necessary to investigate this question.

Previous studies have demonstrated the role of theta oscillations in the attentional exploration of the visual space (Busch & VanRullen, 2010; Dugué, McLelland et al., 2015; Jia, Liu, Fang, & Luo, 2017; Landau et al., 2015; Rollenhagen & Olson, 2005), consistent with the theta periodicity observed here in the invalid condition. Those authors have suggested that the observed behavioral periodicity is due to an intrinsic property of the system—that is, brain oscillations at the theta frequency modulate behavioral performance periodically at the same frequency. A recent psychophysics study explicitly manipulated spatial attentional orienting to assess the behavioral periodicity of attentional sampling with a discrimination task (Song et al., 2014). Such tasks allow assessment of whether the effect of attentional cuing reflects changes in sensory (d') rather than decisional (criterion) processing. On the contrary, in detection tasks the challenge is to disentangle whether higher performance is due to facilitation of information coding at that location, probability matching, or a decision mechanism (see Dugué, Merriam, et al., 2017). The results of the Song et al. study suggest that attention samples information periodically at low frequencies (alpha and theta). Unfortunately, the main dependent variable was reaction time, which can reflect perceptual processing speed, motor anticipation (Correa, Triviño, Pérez-Dueñas, Acosta, & Lupiáñez, 2010), and criterion (Carrasco & McElree, 2001). Here, we explicitly manipulated the reorienting of attention to directly address the following question: Is the periodicity in behavioral performance due to the sequential sampling by attention of the different stimulus locations or to the independent sampling of each location? We measured d' as the main dependent variable and verified that attention in the 2-AFC orientation-discrimination task was successfully manipulated for each participant, with no speed/accuracy trade-off.

Critically, we flashed two stimuli at various delays after the 2-AFC task to probe the state of attentional

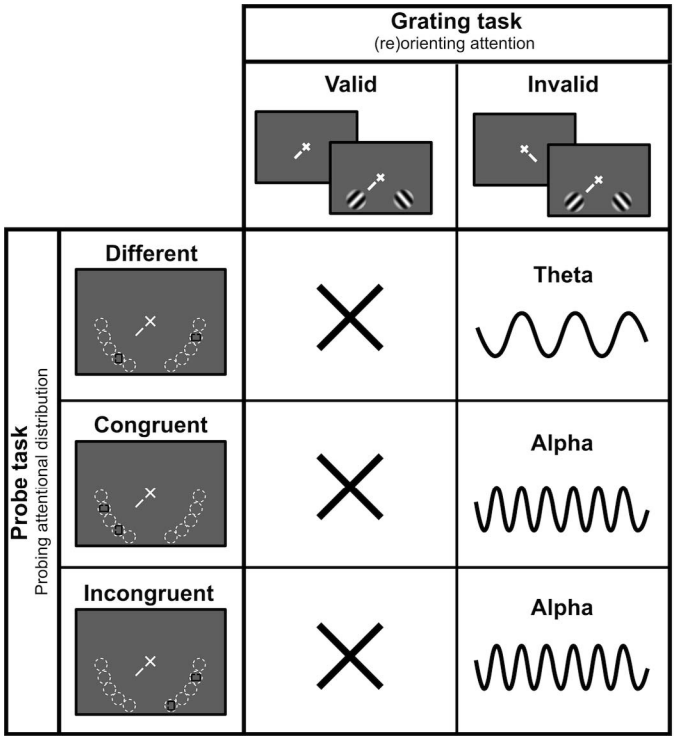

Figure 7. Summary. Attention reorients (invalid, different) periodically between the attended and the unattended location at the theta frequency (~4 Hz), and each stimulus location (invalid, congruent and incongruent) is sampled periodically at the alpha frequency (~11 Hz).

allocation during the course of the trial. Thanks to this manipulation, we argue, the response cue in the invalid condition (i.e., the reorienting signal) did not reorient attention only once but multiple times, with attention periodically switching from one spatial location to another. This surprising result was recently reported by Dugué et al. (2016), who used a similar approach. They used TMS to interfere with the processing of the target and the distractor stimuli independently, at various delays during the same 2-AFC orientation-discrimination task, in order to perturb the orienting or reorienting of attention. They similarly observed that endogenous attention periodically reoriented from the distractor location to the target location (invalid condition) at the theta frequency (~5 Hz). Here, using a psychophysics approach instead of directly interfering with neural processing, we replicated that finding. Our results point to a slightly lower frequency of reorienting—that is, ~4 Hz. This discrepancy might be due to a different temporal resolution between the two studies (i.e., 13 different delays were sampled here, reaching a higher temporal resolution). Taken together, these results suggest that in this specific 2-AFC orientation-discrimination task, attention is not independently sampling each location periodically, but is sequentially sampling the two stimulus positions, alternating from one to the other at the theta frequency.

Interestingly, the specific frequency of attentional exploration, although always in the theta frequency range, varies across studies between 4 and 8 Hz (Busch & VanRullen, 2010; Dugué, McLelland et al., 2015; Dugué, Xue, & Carrasco, 2017; Fiebelkorn et al., 2013; Huang et al., 2015; Landau & Fries, 2012; Landau et al., 2015; Song et al., 2014; van Diepen, Miller, Mazaheri, & Geng, 2016; VanRullen, 2013; VanRullen, Carlson, & Cavanagh, 2007). It is possible that the differences in task parameters could modulate the frequency of the attentional sampling. Recent studies have shown that the peak frequency of alpha oscillations can be shifted depending on task demands or general cognitive load (Haegens, Cousijn, Wallis, Harrison, & Nobre, 2014; Mierau, Klimesch, & Lefebvre, 2017; Wutz, Melcher, & Samaha, 2018). These studies suggest that a top-down modulation of the alpha peak frequency in occipital areas optimizes sensory sampling and interareal communication (see review and model by Mierau et al., 2017). Although these studies do not explicitly suggest a general mechanism that would also be present in other frequency bands—for example, theta—it may be the case that modulation in the theta peak frequency due to task demands and top-down factors could explain differences in the precise peak frequency across studies and tasks.

We found a periodic modulation in the invalid but not in the valid condition—that is, when attention was reoriented but not when it was sustained at the initially cued location—consistent with Dugué et al. (2016). Other studies have shown modulations in the probability of detecting a target in conditions where attention was sustained (Fiebelkorn et al., 2013; Rollenhagen & Olson, 2005; VanRullen et al., 2007), although different types of attention were manipulated. As argued by Dugué et al. (2016), it is possible that sampling in the valid condition may have been similarly modulated but with its own spontaneous phase. In this condition, the orienting process would not have reset the underlying oscillation, and the probes would not bear a phase relation with attention. However, in the invalid condition, the attentional reorienting process would have reset the phase of the oscillation, which could then be revealed by the two probe stimuli. This result challenges the idea that theta oscillations serve as a general attentional rhythm across spatial locations, suggesting that attentional reorienting is crucial to triggering the theta sampling process.

Recently, several studies have investigated the role of microsaccades in brain and behavioral rhythms (Bellet, Chen, & Hafed, 2017; Bosman, Womelsdorf, Desimone, & Fries, 2009; Deouell, 2016; Helfrich, 2017). Specifically, Bellet et al. (2017) recently demonstrated that both the onset time and the direction of micro-

saccades modulate alpha and beta periodic modulations of reaction times in a detection task. Lowet, Roberts, Bosman, Fries, and De Weerd (2016) showed that gamma oscillations in areas V1 and V2 of the monkey brain covaried with a microsaccade-related theta oscillation. Together, these findings suggest that microsaccades may organize visual processing through phase reset of brain oscillations (Deouell, 2016; Helfrich, 2017). Our paradigm did not allow for investigating microsaccades (i.e., a very low number of microsaccades between the offset of the grating stimuli and the onset of the probes, which is where attentional reorienting takes place). Further studies will thus be needed to investigate the link between microsaccades and the observed theta and alpha behavioral rhythms.

Conclusions

Using a probability-estimation approach, we show not only that attentional reorienting samples space periodically at the theta frequency (~4 Hz) but also that each spatial location is sampled periodically at the alpha frequency (~11 Hz) by an ongoing sensory rhythm. Together, these results support the idea that our brain samples information periodically, at low frequencies. Finally, our analysis approach using probability estimation of stimulus identification to probe the state of the attention system is a valuable, sufficiently powered tool to investigate the spatiotemporal dynamics of information processing.

Keywords: alpha, *attention*, *periodicity*, *reorienting*, *sampling*, *theta*

Acknowledgments

The authors thank Ian Donovan for his useful comments on the manuscript. This work was supported by ANR-DFG grants to LD (J18P08ANR00) and NAB (BU 2400/8-1).

Commercial relationships: none.
Corresponding author: Mehdi Senoussi.
Email: senoussi.m@gmail.com.
Address: Department of Experimental Psychology, Ghent University, Ghent, Belgium.

References

Bellet, J., Chen, C.-Y., & Hafed, Z. M. (2017). Sequential hemifield gating of α- and β-behavioral performance oscillations after microsaccades. *Journal of Neurophysiology*, *118*(5), 2789–2805, https://doi.org/10.1152/jn.00253.2017.

Bosman, C. A., Womelsdorf, T., Desimone, R., & Fries, P. (2009). A microsaccadic rhythm modulates gamma-band synchronization and behavior. *The Journal of Neuroscience*, *29*(30), 9471–9480, https://doi.org/10.1523/JNEUROSCI.1193-09.2009.

Busch, N. A., & VanRullen, R. (2010). Spontaneous EEG oscillations reveal periodic sampling of visual attention. *Proceedings of the National Academy of Sciences, USA*, *107*(37), 16048–16053, https://doi.org/10.1073/pnas.1004801107.

Busse, L., Katzner, S., & Treue, S. (2008). Temporal dynamics of neuronal modulation during exogenous and endogenous shifts of visual attention in macaque area MT. *Proceedings of the National Academy of Sciences, USA*, *105*(42), 16380–16385, https://doi.org/10.1073/pnas.0707369105.

Carrasco, M. (2011). Visual attention: The past 25 years. *Vision Research*, *51*(13), 1484–1525, https://doi.org/10.1016/j.visres.2011.04.012.

Carrasco, M. (2014). Spatial attention: Perceptual modulation. In S. Kastner & A. C. Nobre (Eds.), *The Oxford handbook of attention* (pp. 183–230). Oxford, UK: Oxford University Press, https://doi.org/10.1093/oxfordhb/9780199675111.013.004.

Carrasco, M., & McElree, B. (2001). Covert attention accelerates the rate of visual information processing. *Proceedings of the National Academy of Sciences, USA*, *98*(9), 5363–5367, https://doi.org/10.1073/pnas.081074098.

Chaumon, M., & Busch, N. A. (2014). Prestimulus neural oscillations inhibit visual perception via modulation of response gain. *Journal of Cognitive Neuroscience*, *26*(11), 2514–2529, https://doi.org/10.1162/jocn_a_00653.

Cheal, M., & Lyon, D. R. (1991). Central and peripheral precuing of forced-choice discrimination. *Quarterly Journal of Experimental Psychology Section A*, *43*(4), 859–880, https://doi.org/10.1080/14640749108400960.

Chen, A., Wang, A., Wang, T., Tang, X., & Zhang, M. (2017). Behavioral oscillations in visual attention modulated by task difficulty. *Frontiers in Psychology*, *8*, 1630, https://doi.org/10.3389/fpsyg.2017.01630.

Chota, S., Luo, C., Crouzet, S. M., Boyer, L., Kienitz, R., Schmid, M. C., & VanRullen, R. (2018). Rhythmic fluctuations of saccadic reaction time arising from visual competition. *Scientific Reports*,

8(1), 15889, https://doi.org/10.1038/s41598-018-34252-7.

Corbetta, M., Patel, G., & Shulman, G. L. (2008). The reorienting system of the human brain: From environment to theory of mind. *Neuron*, *58*(3), 306–324, https://doi.org/10.1016/j.neuron.2008.04.017.

Correa, Á., Triviño, M., Pérez-Dueñas, C., Acosta, A., & Lupiáñez, J. (2010). Temporal preparation, response inhibition and impulsivity. *Brain and Cognition*, *73*(3), 222–228, https://doi.org/10.1016/j.bandc.2010.05.006.

Davidson, M. J., Alais, D., van Boxtel, J. J. A., & Tsuchiya, N. (2018). Attention periodically samples competing stimuli during binocular rivalry. *BioRxiv* 253740, https://doi.org/10.1101/253740.

Deouell, L. Y. (2016). Microsaccades mediate a bottom-up mechanism for cross-frequency coupling in early visual cortex (Commentary on Lowet et al.). *European Journal of Neuroscience*, *43*(10), 1284–1285, https://doi.org/10.1111/ejn.13181.

Dubois, J., Hamker, F. H., & VanRullen, R. (2009). Attentional selection of noncontiguous locations: The spotlight is only transiently "split." *Journal of Vision*, *9*(5):3, 1–11, https://doi.org/10.1167/9.5.3. [PubMed] [Article]

Dugué, L., Beck, A.-A., Marque, P., & VanRullen, R. (in press). Contribution of FEF to attentional periodicity during visual search: A TMS study. *eNeuro*.

Dugué, L., Marque, P., & VanRullen, R. (2015). Theta oscillations modulate attentional search performance periodically. *Journal of Cognitive Neuroscience*, *27*(5), 945–958, https://doi.org/10.1162/jocn_a_00755.

Dugué, L., McLelland, D., Lajous, M., & VanRullen, R. (2015). Attention searches nonuniformly in space and in time. *Proceedings of the National Academy of Sciences, USA*, *112*(49), 15214–15219, https://doi.org/10.1073/pnas.1511331112.

Dugué, L., Merriam, E. P., Heeger, D. J., & Carrasco, M. (2017). Specific visual subregions of TPJ mediate reorienting of spatial attention. *Cerebral Cortex*, *28*(7), 2375–2390, https://doi.org/10.1093/cercor/bhx140.

Dugué, L., Roberts, M., & Carrasco, M. (2016). Attention reorients periodically. *Current Biology*, *26*(12), 1595–1601, https://doi.org/10.1016/j.cub.2016.04.046.

Dugué, L., & VanRullen, R. (2014). The dynamics of attentional sampling during visual search revealed by Fourier analysis of periodic noise interference. *Journal of Vision*, *14*(2):11, 1–15, https://doi.org/10.1167/14.2.11. [PubMed] [Article]

Dugué, L., & VanRullen, R. (2017). Transcranial magnetic stimulation reveals intrinsic perceptual and attentional rhythms. *Frontiers in Neuroscience*, *11*, 154, https://doi.org/10.3389/fnins.2017.00154.

Dugué, L., Xue, A. M., & Carrasco, M. (2017). Distinct perceptual rhythms for feature and conjunction searches. *Journal of Vision*, *17*(3):22, 1–15, https://doi.org/10.1167/17.3.22. [PubMed] [Article]

Fiebelkorn, I. C., Pinsk, M. A., & Kastner, S. (2018). A dynamic interplay within the frontoparietal network underlies rhythmic spatial attention. *Neuron*, *99*(4), 842–853. e8, https://doi.org/10.1016/j.neuron.2018.07.038.

Fiebelkorn, I. C., Saalmann, Y. B., & Kastner, S. (2013). Rhythmic sampling within and between objects despite sustained attention at a cued location. *Current Biology*, *23*(24), 2553–2558, https://doi.org/10.1016/j.cub.2013.10.063.

Gulbinaite, R., van Viegen, T., Wieling, M., Cohen, M. X., & VanRullen, R. (2017). Individual alpha peak frequency predicts 10 Hz flicker effects on selective attention. *The Journal of Neuroscience*, *37*(42), 10173–10184, https://doi.org/10.1523/JNEUROSCI.1163-17.2017.

Haegens, S., Cousijn, H., Wallis, G., Harrison, P. J., & Nobre, A. C. (2014). Inter- and intra-individual variability in alpha peak frequency. *NeuroImage*, *92*, 46–55, https://doi.org/10.1016/j.neuroimage.2014.01.049.

Helfrich, R. F. (2017). The rhythmic nature of visual perception. *Journal of Neurophysiology*, *119*(4), 1251–1253, https://doi.org/10.1152/jn.00810.2017.

Helfrich, R. F., Fiebelkorn, I. C., Szczepanski, S. M., Lin, J. J., Parvizi, J., Knight, R. T., & Kastner, S. (2018). Neural mechanisms of sustained attention are rhythmic. *Neuron*, *99*(4), 854–865. e5, https://doi.org/10.1016/j.neuron.2018.07.032.

Helfrich, R. F., Huang, M., Wilson, G., & Knight, R. T. (2017). Prefrontal cortex modulates posterior alpha oscillations during top-down guided visual perception. *Proceedings of the National Academy of Sciences, USA*, *114*(35), 9457–9462, https://doi.org/10.1073/pnas.1705965114.

Ho, H. T., Leung, J., Burr, D. C., Alais, D., & Morrone, M. C. (2017). Auditory sensitivity and decision criteria oscillate at different frequencies separately for the two ears. *Current Biology*, *27*(23), 3643–3649. e3, https://doi.org/10.1016/j.cub.2017.10.017.

Huang, Y., Chen, L., & Luo, H. (2015). Behavioral oscillation in priming: Competing perceptual predictions conveyed in alternating theta-band rhythms. *The Journal of Neuroscience*, *35*(6), 2830–

2837, https://doi.org/10.1523/JNEUROSCI.4294-14.2015.

Jia, J., Liu, L., Fang, F., & Luo, H. (2017). Sequential sampling of visual objects during sustained attention. *PLOS Biology*, *15*(6), e2001903, https://doi.org/10.1371/journal.pbio.2001903.

Kienitz, R., Schmiedt, J. T., Shapcott, K. A., Kouroupaki, K., Saunders, R. C., & Schmid, M. C. (2018). Theta rhythmic neuronal activity and reaction times arising from cortical receptive field interactions during distributed attention. *Current Biology*, *28*(15), 2377–2387. e5, https://doi.org/10.1016/j.cub.2018.05.086.

Klimesch, W. (2018). The frequency architecture of brain and brain body oscillations: An analysis. *European Journal of Neuroscience*, *48*(7), 2431–2453, https://doi.org/10.1111/ejn.14192.

Landau, A. N., & Fries, P. (2012). Attention samples stimuli rhythmically. *Current Biology*, *22*(11), 1000–1004, https://doi.org/10.1016/j.cub.2012.03.054.

Landau, A. N., Schreyer, H. M., van Pelt, S., & Fries, P. (2015). Distributed attention is implemented through theta-rhythmic gamma modulation. *Current Biology*, *25*(17), 2332–2337, https://doi.org/10.1016/j.cub.2015.07.048.

Liu, T., Stevens, S. T., & Carrasco, M. (2007). Comparing the time course and efficacy of spatial and feature-based attention. *Vision Research*, *47*(1), 108–113, https://doi.org/10.1016/j.visres.2006.09.017.

Lowet, E., Roberts, M. J., Bosman, C. A., Fries, P., & De Weerd, P. (2016). Areas V1 and V2 show microsaccade-related 3–4-Hz covariation in gamma power and frequency. *European Journal of Neuroscience*, *43*(10), 1286–1296, https://doi.org/10.1111/ejn.13126.

Mierau, A., Klimesch, W., & Lefebvre, J. (2017). State-dependent alpha peak frequency shifts: Experimental evidence, potential mechanisms and functional implications. *Neuroscience*, *360*, 146–154, https://doi.org/10.1016/j.neuroscience.2017.07.037.

Müller, H. J., & Rabbitt, P. M. (1989). Reflexive and voluntary orienting of visual attention: Time course of activation and resistance to interruption. *Journal of Experimental Psychology: Human Perception and Performance*, *15*(2), 315–330, https://doi.org/10.1037/0096-1523.15.2.315.

Nakayama, K., & Mackeben, M. (1989). Sustained and transient components of focal visual attention. *Vision Research*, *29*(11), 1631–1647, https://doi.org/10.1016/0042-6989(89)90144-2.

Pestilli, F., Ling, S., & Carrasco, M. (2009). A population-coding model of attention's influence on contrast response: Estimating neural effects from psychophysical data. *Vision Research*, *49*(10), 1144–1153, https://doi.org/10.1016/j.visres.2008.09.018.

Posner, M. I. (1988). Structures and function of selective attention. In T. Boll & B. K. Bryant (Eds.), *Clinical neuropsychology and brain function: Research, measurement, and practice* (pp. 173–202). Washington, DC: American Psychological Association, https://doi.org/10.1037/10063-005.

Rollenhagen, J. E., & Olson, C. R. (2005). Low-frequency oscillations arising from competitive interactions between visual stimuli in macaque inferotemporal cortex. *Journal of Neurophysiology*, *94*(5), 3368–3387, https://doi.org/10.1152/jn.00158.2005.

Rosanova, M., Casali, A., Bellina, V., Resta, F., Mariotti, M., & Massimini, M. (2009). Natural frequencies of human corticothalamic circuits. *The Journal of Neuroscience*, *29*(24), 7679–7685, https://doi.org/10.1523/JNEUROSCI.0445-09.2009.

Sokoliuk, R., Mayhew, S. D., Aquino, K., Wilson, R., Brookes, M. J., Francis, S. T., … Mullinger, K. J. (2018). Two spatially distinct posterior alpha sources fulfill different functional roles in attention. *BioRxiv*, 384065, https://doi.org/10.1101/384065.

Song, K., Meng, M., Chen, L., Zhou, K., & Luo, H. (2014). Behavioral oscillations in attention: Rhythmic α pulses mediated through θ band. *The Journal of Neuroscience*, *34*(14), 4837–4844, https://doi.org/10.1523/JNEUROSCI.4856-13.2014.

Spyropoulos, G., Bosman, C. A., & Fries, P. (2018). A theta rhythm in macaque visual cortex and its attentional modulation. *Proceedings of the National Academy of Sciences, USA*, *115*(24), E5614–E5623, https://doi.org/10.1073/pnas.1719433115.

van Diepen, R. M., Miller, L. M., Mazaheri, A., & Geng, J. J. (2016). The role of alpha activity in spatial and feature-based attention. *eNeuro*, *3*(5), https://doi.org/10.1523/ENEURO.0204-16.2016.

VanRullen, R. (2013). Visual attention: A rhythmic process? *Current Biology*, *23*(24), R1110–R1112, https://doi.org/10.1016/j.cub.2013.11.006.

VanRullen, R. (2016). Perceptual cycles. *Trends in Cognitive Sciences*, *20*(10), 723–735, https://doi.org/10.1016/j.tics.2016.07.006.

VanRullen, R., Carlson, T., & Cavanagh, P. (2007). The blinking spotlight of attention. *Proceedings of the National Academy of Sciences, USA*, *104*(49), 19204–19209, https://doi.org/10.1073/pnas.0707316104.

Wutz, A., Melcher, D., & Samaha, J. (2018). Frequency modulation of neural oscillations according to visual task demands. *Proceedings of the National*

Academy of Sciences, USA, *115*(6), 1346–1351, https://doi.org/10.1073/pnas.1713318115.

Zhang, H., Morrone, M. C., & Alais, D. (2019). Behavioural oscillations in visual orientation discrimination reveal distinct modulation rates for both sensitivity and response bias. *Scientific Reports*, *9*(1), 1115, https://doi.org/10.1038/s41598-018-37918-4.